Inorg. Chem. **2002**, *41*, 4502–4508

A Family of Vanadate Esters of Monoionized and Diionized Aromatic 1,2-Diols: Synthesis, Structure, and Redox Activity

Bharat Baruah,[†] Samir Das,[†] and Animesh Chakravorty*[,†,‡]

Department of Inorganic Chemistry, Indian Association for the Cultivation of Science, Kolkata 700 032, India, and Jawaharlal Nehru Centre for Advanced Scientific Research, Bangalore 560 064, India

Received April 4, 2002

The concerned diols (general abbreviation, H_2L) are catechol (H_2L^1) and its 3,5-Bu^t_2 derivative (H_2L^2). Esters of the type VO(xsal)(HL), **2**, are obtained by reacting H_2L with VO(xsal)(H_2O) or VO(xsal)(OMe)(HOMe), where $xsal^{2-}$ is the diionized salicylaldimine of glycine (x = g), L-alanine (x = a), or L-valine (x = v). The reaction of $VO(acac)_2$ with H_2L and the salicylaldimine (Hpsal) of 2-picolylamine has furnished VO(psal)(L), **3**. In the structures of VO(gsal)(HL^1), **2a**, and VO(vsal)(HL^2), **2f**, the HL^- ligand is O,O-chelated, the phenolic oxygen lying trans to the oxo oxygen atom. The $xsal^{2-}$ coligand has a folded structure and the conformation of **2f** is exclusively endo. In both **2a** and **2f** the phenolic oxygen atom is strongly hydrogen bonded (O···O, 2.60 Å) to a carboxylic oxygen atom of a neighboring molecule. In VO(psal)(L^2)·H_2O, **3b**, the diionized diol is O,O-chelated to the metal and the water molecule is hydrogen bonded to a phenoxidic oxygen atom (O···O, 2.84 Å). The C–O and C–C distances in the V(diol) fragment reveal that **2** is a pure catecholate and **3** is a catecholate–semiquinonate hybrid. In solution each ester gives rise to a single ^{51}V NMR signal (no diastereoisomers), which generally shifts downfield with a decrease in the ester LMCT band energy. The V(V)/V(IV) and catecholate–semiquinonate reduction potentials lie near –0.75 and 0.35, and 1.10 and 0.70 V vs SCE for **2** and **3**, respectively. Molecular oxygen reacts smoothly with **2** quantitatively furnishing the corresponding *o*-quinone, and in the presence of H_2L the reaction becomes catalytic. In contrast, type **3** esters are inert to oxygen. The initial binding of O_2 to **2** is proposed to occur via hydrogen bonding with chelated HL^-.

Introduction

The binding of vanadium to aromatic 1,2-diols[1] has been of interest in contexts such as analytical color reactions,[2] tunicate chemistry,[3] and diol oxidation.[4−6] Synthetic and structural studies have demonstrated that the common diol coordination mode is O,O-chelation in the diionized form to trivalent,[7,8] tetravalent[7,9,10] and pentavalent[10−12] vanadium. Variants include semiquinonate and phenolato-bridged types.[4,13]

Monoionized aliphatic diols[14,15] including modified car-

* To whom correspondence should be addressed at the Indian Association for the Cultivation of Science. E-mail: icac@mahendra.iacs.res.in.

[†] Indian Association for the Cultivation of Science.

[‡] Jawaharlal Nehru Centre for Advanced Scientific Research.

(1) (a) Pierpont, C. G.; Lange, C. W. *Prog. Inorg. Chem.* **1994**, *41*, 331. (b) Pierpont, C. G.; Buchanan, R. M. *Coord. Chem. Rev.* **1981**, *38*, 45.

(2) (a) Nardillo, A. M.; Catoggio, J. A. *Anal. Chim. Acta* **1975**, *74*, 85. (b) Lobinski, R.; Marczenko, Z. *Anal. Chim. Acta* **1989**, *226*, 281.

(3) (a) Michibata, H.; Sakurai, H. In *Vanadium in Biological Systems*; Chasteen, N. D., Ed.; Kluwer Academic Publisher: Dordrecht, The Netherlands, 1990; pp 153−171. (b) Smith, M. J.; Kim, D.; Horenstein, B.; Nakanishi, K.; Kustin, K. *Acc. Chem. Res.* **1991**, *24*, 117.

(4) Cass, M. E.; Greene, D. L.; Buchanan, R. M.; Pierpont, C. G. *J. Am. Chem. Soc.* **1983**, *105*, 2680.

(5) (a) Galeffi, B.; Postel, M.; Grand, A.; Rey, P. *Inorg. Chim. Acta* **1989**, *160*, 87. (b) Galeffi, B.; Postel, M.; Grand, A.; Rey, P. *Inorg. Chim. Acta* **1987**, *129*, 1. (c) Tatsuno, Y.; Tatsuda, M.; Otsuka, S. *J. Chem. Soc., Chem. Commun.* **1982**, 1101. (d) Tatsuno, Y.; Tatsuda, M.; Otsuka, S.; Tani, K. *Inorg. Chim. Acta* **1983**, *104*, 79. (e) Tatsuno, Y.; Tatsuda, M.; Otsuka, S.; Tani, K. *Chem. Lett.* **1984**, 1209. (f) Tatsuno, Y.; Nakamura, C.; Saito, T. *J. Mol. Catal.* **1987**, *42*, 57. (g) Nishida, Y.; Kikuchi, H. *Z. Naturforsch.* **1989**, *44b*, 245. (h) Casellato, U.; Tamburini, S.; Vigato, P. A.; Vidali, M.; Fenton, D. E. *Inorg. Chim. Acta* **1984**, *84*, 101. (i) Roman, E.; Tapia, F.; Barrera, M.; Garland, M.-T.; LeMarouille, J.-Y.; Giannotti, C. *J. Organomet. Chem.* **1985**, *C8*, 297.

(6) Preliminary communication based on hydrazone coligand: Rath, S. P.; Rajak, K. K.; Chakravorty, A. *Inorg. Chem.* **1999**, *38*, 4376.

(7) Cooper, S. R.; Koh, Y. B.; Raymond, K. N. *J. Am. Chem. Soc.* **1982**, *104*, 5092.

(8) Bulls, A. R.; Pippin, C. G.; Hahn, F. E.; Raymond, K. N. *J. Am. Chem. Soc.* **1990**, *112*, 2627.

(9) (a) Simpson, C. L.; Pierpont, C. G. *Inorg. Chem.* **1992**, *31*, 4308. (b) Dewey, T. M.; Bois, J. D.; Raymond, K. N. *Inorg. Chem.* **1993**, *32*, 1729.

10.1021/ic020259d CCC: $22.00
Published on Web 08/01/2002

bohydrates[16] have been shown to chelate VO^{3+} forming esters of type **1** where the chelate ring is five- or six-membered and the vacant sites are engaged by a tridentate coligand. This has prompted us to search for **2**, the aromatic ester analogue of **1**, and herein we report the isolation and

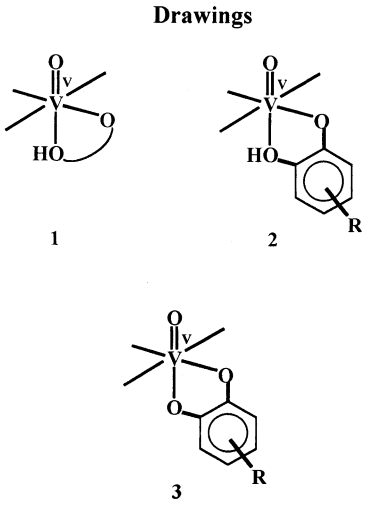

characterization of a family of this type incorporating salicylaldimines of achiral and chiral α-amino acids as coligands.[6] For comparison, diionized diol chelates of type **3** also bearing a salicylaldimine coligand have also been prepared. Structure determination has revealed that while the diol ligand in **2** has model catechol character, it is significantly semiquinonoid in **3**. The distinctive spectral and electrochemical features of **2** and **3** and the spontaneous solution reactivity toward oxygen, a property exclusive to **2**, are scrutinized.

Results and Discussion

(A) Diols, Coligands, and Vanadate Esters. (a) Synthesis. The aromatic diol ligands (general abbreviation, H_2L) used are catechol, H_2L^1, and 3,5-di(*tert*-butyl)catechol, H_2L^2. The salicylaldimines of glycine, L-alanine, and L-valine, **4a**−**c** (general abbreviation, H_2xsal) and of 2-picolylamine, **5**, are employed as coligands. Upon reacting $V^{IV}O(xsal)(H_2O)$[17] or $V^{V}O(xsal)(OMe)(HOMe)$[18] with a slight excess of H_2L in methanol or acetonitrile at room temperature in air violet to blue solutions are formed which afford $V^{V}O(xsal)(HL)$ as dark crystalline solids in excellent yields. Violet $V^{V}O(psal)(L)$ was conveniently isolated by the stoichiometric reactions of $VO(acac)_2$[19] with Hpsal and H_2L in methanol under ambient conditions.

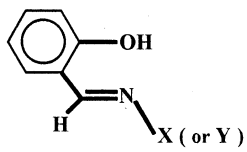

4a, X = CH_2CO_2H — H_2gsal

4b, X = $CH(Me)CO_2H$ — H_2asal

4c, X = $CH(CHMe_2)CO_2H$ — H_2vsal

5, Y = $CH_2C_5H_4N$ — Hpsal

Six esters of the type VO(xsal)(HL), **2a**−**f**, and two of the type VO(psal)(L), **3a**,**b** (the latter occurring as a hydrate), have been isolated (Table 1). Monoionized aromatic 1,2-diol chelation as in **2** is rare in transition metal chemistry. A notable example, relevant to catechol dioxygenase activity,[20] occurs in iron(II) chemistry.[21]

(b) Spectral Characterization of the Esters. The type **2** species are characterized by a relatively broad OH stretch (2450−2580 cm^{-1}) suggesting the presence of strong hydrogen bonding. In ^1H NMR the OH resonance (near 10 ppm) is very broad and is not observable in all cases. The compounds display moderately strong (ϵ 3000−5000 M^{-1} cm^{-1}) absorption in the visible region: one band near 600 nm in **2** and two bands near 540 and 850 nm in **3** (Table 1). In general the absorption shifts to lower energies in going from $(HL^1)^-$ to $(HL^2)^-$ and $(L^1)^{2-}$ to $(L^2)^{2-}$ esters (Table 1) consistent with $p\pi$ $(HL^-/L^{2-}) \rightarrow$ d (V) LMCT assignment.

The ^{51}V chemical shifts of the esters are listed in Table 1. Each ester gives rise to a single signal even for the type **2**

Table 1. Band Maxima in the Visible Region[a] and ^{51}V NMR Chemical Shifts[b]

compd	number	band position (λ_{max}, nm)	^{51}V NMR (δ, ppm)
$VO(gsal)(HL^1)$	**2a**	578	−460
$VO(asal)(HL^1)$	**2b**	591	−457
$VO(vsal)(HL^1)$	**2c**	602	−455
$VO(gsal)(HL^2)$	**2d**	638	−416
$VO(asal)(HL^2)$	**2e**	641	−414
$VO(vsal)(HL^2)$	**2f**	647	−410
$VO(psal)(L^1)$	**3a**	850, 525	270
$VO(psal)(L^2)\cdot H_2O$	**3b**	855, 550	462

[a] The solvent is Me_2CO. [b] The solvent is $(CD_3)_2SO$ for **2a**−**2f** and $CDCl_3$ for **3a**,**b**.

(10) Kabanos, T. A.; White, A. J. P.; William, D. J.; Woollians, J. D. *J. Chem. Soc., Chem. Commun*. **1992**, 17.
(11) (a) Cass, M. E.; Gordon, N. R.; Pierpont, C. G. *Inorg. Chem.* **1986**, *25*, 3962. (b) Kabanos, T. A.; Slawin, A. M. Z.; Williams, D. J.; Woollians, J. D. *J. Chem. Soc., Chem. Commun*. **1990**, 193.
(12) (a) Cornman, C. R.; Colpas, G. J.; Hoeschele, J. D.; Kampf, J.; Pecoraro, V. L. *J. Am. Chem. Soc.* **1992**, *114*, 9925. (b) Cornman, C. R.; Kampf, J.; Pecoraro, V. L. *Inorg. Chem.* **1992**, *31*, 1981.
(13) (a) Mazzanti, M.; Floriani, C.; Chiesi-Villa, A.; Guastini, C. *J. Chem. Soc., Dalton Trans*. **1989**, 1793. (b) Manos, M. J.; Tasiopoulos, A. J.; Raptopoulou, C.; Terzis, A.; Woollians, J. D.; Slawin, A. M. Z.; Keramidas, A. D.; Kabanos, T. A. *J. Chem. Soc., Dalton Trans*. **2001**, 1556.
(14) (a) Mondal, S.; Rath, S. P.; Dutta, S.; Chakravorty, A. *J. Chem. Soc., Dalton. Trans.* **1996**, 99. (b) Mondal, S.; Ghosh, P.; Chakravorty, A. *Indian J. Chem.* **1996**, *35A*, 171. (c) Rath, S. P.; Mondal, S.; Chakravorty, A. *Inorg. Chim. Acta* **1997**, *263*, 247.
(15) (a) Mondal, S.; Rath, S. P.; Rajak, K. K.; Chakravorty, A. *Inorg. Chem.* **1998**, *37*, 1713. (b) Rath, S. P.; Rajak, K. K.; Mondal, S.; Chakravorty, A. *J. Chem. Soc., Dalton Trans.* **1998**, 2097.
(16) (a) Rajak, K. K.; Rath, S. P.; Mondal, S.; Chakravorty, A. *Inorg. Chem.* **1999**, *38*, 3283. (b) Rajak, K. K.; Rath, S. P.; Mondal, S.; Chakravorty, A. *Indian J. Chem*. **1999**, *38A*, 405. (c) Rajak, K. K.; Rath, S. P.; Mondal, S.; Chakravorty, A. *J. Chem. Soc., Dalton Trans.* **1999**, 2537. (d) Rajak, K. K.; Baruah, B.; Rath, S. P.; Chakravorty, A. *Inorg. Chem.* **2000**, *39*, 1598.
(17) Theriot, L. J.; Carlisle, G. O.; Hu, H. J. *J. Inorg. Nucl. Chem.* **1969**, *31*, 2841.
(18) (a) Dutta, S.; Mondal, S.; Chakravorty, A. *Polyhedron* **1995**, *14*, 1163. (b) Nakajima, K.; Kojima, M.; Toriumi, K.; Saito, K.; Fujita, J. *Bull. Chem. Soc. Jpn.* **1989**, *62*, 760.
(19) Rowe, R. A.; Jones, M. M. *Inorg. Synth*. **1957**, *5*, 133.
(20) Kruger, H.-J. In *Biomemetic Oxidations Catalysed by Transition Metal Complexes*; Meunier, B., Ed.; Imperial College Press: London, UK, 2000; pp 363−413.
(21) (a) Chiou, Y.-M.; Que, L., Jr. *Inorg. Chem.* **1995**, *34*, 3577. (b) Shu, L.; Chiou, Y.-M.; Orville, A. M.; Miller, M. A.; Lipscomb, J. D.; Que, L., Jr. *Biochemistry* **1995**, *34*, 6649.

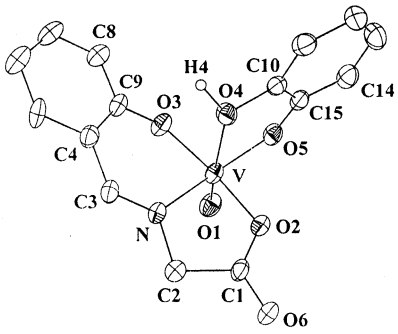

Figure 1. Perspective view and atom-labeling scheme of VO(gsal)(HL^1), **2a**. All non-hydrogen atoms are represented by their 30% probability ellipsoids.

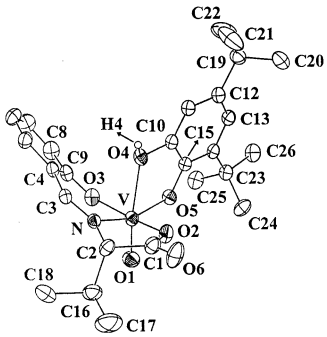

Figure 2. Perspective view and atom-labeling scheme of VO(vsal)(HL^2), **2f**. All non-hydrogen atoms are represented by their 30% probability ellipsoids.

species bearing chiral amino acid residues, suggesting[15a] that their solutions contain only one diastereoisomer as in the solid state, vide infra. Similarly each proton type gives rise to a single ^{1}H NMR signal (see Experimental Section). The ^{51}V signals generally shift[12a] downfield as the average LMCT band energy decreases as between **2a** and **2d** (40 ppm), between **3a** and **3b** (190 ppm), and between **2a** and **3a** (730 ppm). In the context of the very large shift between type **2** and type **3** species it is significant that in **2** the diol ligand is catecholate in character while in **3** there is very significant semiquinone contribution, vide infra.

(B) Structures. (a) $(HL)^-$ Esters. The structures of VO(gsal)(HL^1), **2a**, and VO(vsal)(HL^2), **2f**, have been determined and molecular views are shown in Figures 1 and 2. Selected bond parameters are listed in Table 2.

In the distorted octahedral VO_5N coordination sphere the metal atom is displaced toward the O(1) atom from the equatorial plane of O(2), O(3), O(5), and N atoms by ~0.35 Å in both **2a** and **2f**. The V−O bond lengths span the range 1.58−2.40 Å, the shortest and the longest being V−O(1) and V−O(4), respectively, lying trans to each other. The phenoxidic oxygen O(5) of HL^- is more strongly coordinated than the phenoxidic oxygen O(3) of $xsal^{2-}$.

The meridionally disposed tridentate ligand is made up of two planar segments (mean deviation, ~0.02 Å) viz. OC_6H_4CHN and CCO_2. The dihedral angle between them is 37.3° in **2a** and 49.9° in **2f**. In VO(xsal) esters of monoionized aliphatic diols the angle spans[14−16] the range 26−40°. The V(HL^1) fragment in **2a** and V(HL^2) fragment (minus Bu^t groups) in **2f** are planar (mean deviation 0.04 Å).

Table 2. Selected Bond Distance (Å) and Angles (deg) for VO(gsal)(HL^1), **2a**, and VO(vsal)(HL^2), **2f**

	2a	**2f**
	distances	
V−O(1)	1.576(3)	1.592(3)
V−O(2)	1.966(3)	1.979(3)
V−O(3)	1.855(3)	1.865(3)
V−O(4)	2.399(3)	2.352(3)
V−O(5)	1.827(3)	1.843(3)
V−N	2.063(4)	2.087(3)
O(4)−C(10)	1.366(5)	1.366(4)
O(5)−C(15)	1.345(5)	1.349(5)
C(10)−C(11)	1.372(7)	1.370(6)
C(10)−C(15)	1.402(6)	1.387(5)
C(11)−C(12)	1.386(7)	1.404(5)
C(12)−C(13)	1.376(8)	1.396(6)
C(13)−C(14)	1.377(8)	1.396(6)
C(14)−C(15)	1.387(7)	1.411(5)
	angles	
O(1)−V−O(2)	98.7(2)	95.5(2)
O(1)−V−O(3)	99.5(2)	99.7(2)
O(1)−V−O(4)	175.5(2)	173.31(14)
O(1)−V−O(5)	100.3(2)	100.9(2)
O(2)−V−O(4)	81.93(13)	80.63(12)
O(3)−V−O(2)	156.86(14)	157.85(13)
O(3)−V−O(4)	80.95(14)	85.58(12)
O(5)−V−O(2)	88.50(14)	93.04(12)
O(5)−V−O(3)	102.0(2)	99.76(13)
O(5)−V−O(4)	75.32(13)	74.00(11)
O(1)−V−N	103.0(2)	106.1(2)
O(2)−V−N	76.73(14)	75.43(13)
O(3)−V−N	85.4(2)	84.88(13)
O(5)−V−N	154.0(2)	151.46(13)
N−V−O(4)	81.46(13)	78.35(11)

In **2f** the V═O bond lies endo to the C(2)−C(16) bond of the chiral amino acid residue (Figure 2). The signs of the atomic coordinates of **2f** were chosen so as to conform the *S* configuration of the L-amino acid residue. Viewed down the V═O axis the equatorial atoms span clockwise when ordered according to their priority sequence[22] O(2) > O(5) > O(3) > N. The absolute configuration of the endo form is thus *CS*. The *AS* diastereoisomer (exo form) is not observed either in the solid state or in solution (vide supra). The chiral preference of the metal site is of steric origin and can be related to the nonplanarity of the $xsal^{2-}$ ligand.[15a]

(b) $(L)^{2-}$ Esters. A molecular view of **3b** is shown in Figure 3 and selected bond parameters are listed in Table 3. The metal atom is displaced by 0.28 Å toward the O(1) atom from the equatorial plane of N(1), N(2), O(2), and O(4). The $psal^-$ ligand is made up of two planar parts (mean deviation, ~0.02 Å) C(1)−C(6), N(1) and C(7)−C(13), O(2), N(2), the dihedral angle between them being 19.7°. The V(L^2) fragment (minus Bu^t groups) is a virtually perfect plane (mean deviation <0.01 Å). The phenoxidic V−O(2) and V−O(4) distances are ~0.03 Å longer than the corresponding distances (V−O(3) and V−O(5), respectively) in **2f**. The phenoxidic V−O(3) bond lying trans to V−O(1) is relatively long but it is still shorter by 0.22 Å than the corresponding phenolic bond V−O(4)H in **2f**.

(c) Nature of the Chelated Diol. The C(10)−O(4) and C(15)−O(5) distances in the V(HL^2) fragment of **2f** are 1.366(4) and 1.349(5) Å, respectively. The aromatic C−C

(22) *Nomenclature of Inorganic Chemistry*; Leigh, G. J., Ed.; Blackwell Scientific Publications: Oxford, UK, 1990; pp 186−187.

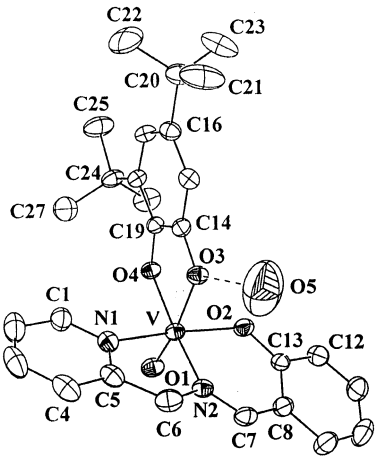

Figure 3. Perspective view and atom-labeling scheme of VO(psal)(L^2)·H_2O, **3b**. All non-hydrogen atoms are represented by their 30% probability ellipsoids.

Table 3. Selected Bond Distances (Å) and Angles (deg) for VO(psal)(L^2)·H_2O, **3b**

distance		angles	
V−O(1)	1.572(3)	O(1)−V−O(4)	97.32(14)
V−O(2)	1.898(3)	O(1)−V−O(2)	99.4(2)
V−O(3)	2.134(3)	O(4)−V−O(2)	98.76(13)
V−O(4)	1.861(3)	O(1)−V−N(2)	101.5(2)
V−N(1)	2.099(4)	O(4)−V−N(2)	159.38(13)
V−N(2)	2.044(3)	O(2)−V−N(2)	86.38(14)
O(3)−C(14)	1.275(5)	O(1)−V−N(1)	94.2(2)
O(4)−C(19)	1.319(4)	O(4)−V−N(1)	93.40(13)
C(14)−C(15)	1.385(6)	O(2)−V−N(1)	160.36(14)
C(15)− C(16)	1.364(6)	N(2)−V−N(1)	77.1(2)
C(16)−C(17)	1.392(6)	O(1)−V−O(3)	172.29(14)
C(17)−C(18)	1.366(6)	O(4)−V−O(3)	76.93(12)
C(18)−C(19)	1.398(5)	O(2)−V−O(3)	86.63(13)
C(14)−C(19)	1.403(6)	N(2)−V−O(3)	83.50(13)
		N(1)−V−O(3)	81.14(13)

lengths (Table 2) are normal. The ligand is thus chelated in the catecholate form. The expected C−O lengths in catecholate and semiquinonate forms are 1.35 and 1.29 Å, respectively.[1,6,23,24] The V(HL^1) fragment in **2a** is very similar (Table 2).

In contrast, the V(L^2) fragment in **3b** is a resonance hybrid of the catecholate (specified as $V^V(L_C^2)$) and semiquinonate ($V^{IV}(L_S^2)$) canonical forms. The C(14)−O(3) and C(19)−O(4) distances are 1.275(5) and 1.314(4) Å, respectively. The C(15)−C(16) and C(17)−C(18) bonds (average length 1.36 Å) are significantly shorter than the other four C−C bonds (average, length 1.39 Å), Table 3. Semiquinone contribution has earlier been documented in two other VO(L) salicylaldimine chelates.[12a]

In summary, the coligand controls the protic and electronic nature of the metal-diol fragment. In **2** the diionized salicylaldimine ($xsal^{2-}$) stabilizes the monoionized catecholate form. In **3** the monoionized salicylaldimine ($psal^-$) promotes diol diionization attended with internal fractional electron transfer expressed in the form of a $V^{IV}(L_S)$ contribution.

(23) Carngo, O.; Castellani, C. B.; Djinovic, K.; Rizzi, M. *J. Chem. Soc., Dalton Trans.* **1992**, 837.
(24) Bag, N.; Lahiri, G. K.; Basu, P.; Chakravorty, A. *J. Chem. Soc., Dalton Trans*. **1992**, 113.

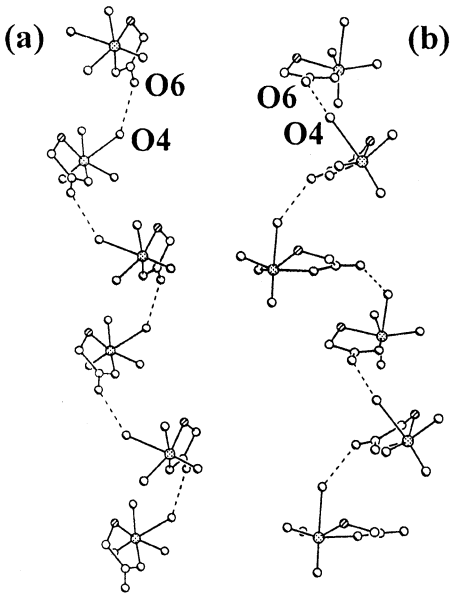

Figure 4. Hydrogen bonding in crystalline (a) VO(gsal)(HL^1), **2a**, and (b) VO(vsal)(HL^2), **2f**, represented in ball-and-stick form (selected atoms only).

Table 4. Electrochemical Data in MeCN

esters	$E_{1/2}$, V[a] (ΔE_p, mV)[b]	E_{pa}, V[c]
VO(gsal)(HL^1), **2a**	−0.60(80)	1.02
VO(asal)(HL^1), **2b**	−0.77(300)	1.10
VO(vsal)(HL^1), **2c**	−0.78(260)	1.12
VO(gsal)(HL^2), **2d**	−0.73(180)	0.98
VO(asal)(HL^2), **2e**	−0.84(320)	1.08
VO(vsal)(HL^2), **2f**	−0.81(180)	1.04
VO(psal)(L^1), **3a**	−0.29(100)	0.76
VO(psal)(L^2)·H_2O, **3b**	−0.40(160)	0.66

[a] Calculated as the average of anodic and cathodic peak potentials. [b] Peak-to-peak separation. [c] Anodic peak potential.

(d) Hydrogen Bonding. Many of the hydrogen atoms of **2a** and **2f** were directly observed in difference Fourier maps, and those include the crucial phenolic hydrogen atoms which are explicity shown in Figures 1 and 2. The O(4) atom is strongly hydrogen bonded to the uncoordinated carboxyl oxygen atom, O(6), of a neighboring molecule (O(4)···O(6), 2.596(5) Å in **2a** and 2.582(5) Å in **2f**), thus generating infinite chains (Figure 4).

In **3b** hydrogen bonding occurs between the phenoxidic O(3) atom and the aqua O(5) atom forming discrete hydrated molecules, Figure 3. The bonding (O(3)···O(5), 2.836(4) Å) is significantly weaker than those in **2a** and **2f**.

(C) Redox Activity. (a) Cyclic Voltammetry. Both **2** and **3** display a quasireversible reductive one-electron response vanadium(V)/vanadium(IV) at negative potentials and a virtually irreversible oxidative response catecholate/semiquinonate at positive potentials. Reduction potential data are listed in Table 4 and a pair of representative voltammograms are displayed in Figure 5. The two responses occur respectively at more negative and more positive potentials in **2** compared to those in **3**. The processes are thus thermodynamically less favorable in **2** than in **3**, consistent with both the higher level of ligand protonation in **2** and the contribution of the $V^{IV}(L_S)$ form to the ground state in **3**.

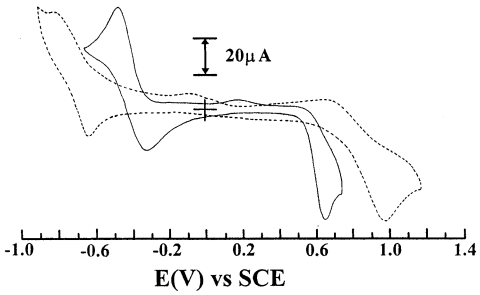

Figure 5. Cyclic voltammograms of (- - -) VO(gsal)(HL^2), **2d**, and (−) VO(psal)(L^2)·H_2O, **3b**, in MeCN.

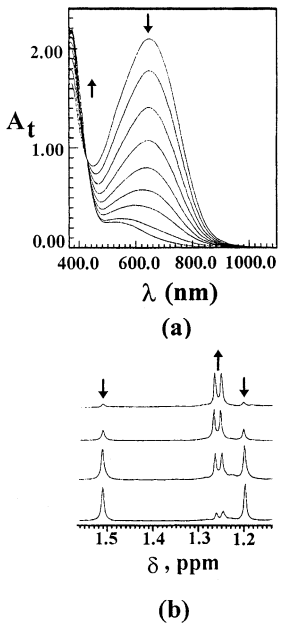

Figure 6. (a) Time evolution spectra (visible region) of VO(vsal)(HL^2), **2f**, in O_2-saturated acetone solution at 295 K (A_t is absorbance). (b) Time evolution of *tert*-butyl signals in **2f** in O_2-saturated acetone-d_6. The signals at δ 1.25 and 1.26 due to free Lq^2 and those at δ 1.19 and 1.51 due to coordinated $(HL^2)^-$ respectively grow and decay with time.

Finally, the vanadium(V)/vanadium(IV) response in aliphatic species of type **1** incorporating $xsal^{2-}$ coligands lies near −0.25 V.[14,15] The aromatic diol in **2** thus promotes superior redox stability to vanadium(V).

(b) Reaction with Oxygen. The VO(xsal)(HL) esters are stable in the solid state under ambient conditions. Their dark solutions, which are otherwise stable, get progressively bleached in the presence of oxygen. The only products isolated from the yellowish brown solutions are the dimeric vanadyl chelate $V_2O_3(xsal)_2$[18b] and the *o*-quinone corresponding to the $(HL)^-$ ligand. The reaction has been quantitated in the case of VO(vsal)(HL^2) in acetone solution. The experimentally determined mass balance corresponds to eq 1. The progress of the reaction is observable in both electronic and ^1H NMR spectra (Figure 6). In oxygen-

$$2VO(vsal)(HL^2) + O_2 \rightarrow V_2O_3(vsal)_2 + 2Lq^2 + H_2O \quad (1)$$

saturated acetone the pseudo-first-order rate constant is found to be 5.64×10^{-4} s^{-1} at 295 K.

Upon adding free H_2L^2 to the solution during the reaction or after its completion the ester is regenerated to the original level and the reaction of eq 1 can start over again. A catalytic cycle for the oxidation of H_2L^2 into Lq^2 by oxygen, eq 3, is readily realized by combining the two reactions. It is an unusual catecholase reaction in which the active

$$V_2O_3(vsal)_2 + 2H_2L^2 \rightarrow 2VO(vsal)(HL^2) + H_2O \quad (2)$$

$$2H_2L^2 + O_2 \rightarrow 2\,Lq^2 + 2H_2O \quad (3)$$

intermediate, VO(vsal)(HL^2), and the catalyst, $V_2O_3(vsal)_2$, are vanadium complexes. In biological catecholase reactions the active sites are generally copper based.[25] Vanadium(III, IV, V) species have been documented to mediate the oxidation of 1,2-diphenols giving mixtures of products including semiquinone, quinone, muconic acid anhydride, and 2-pyrone.[4,5] Vanadium-promoted clean catecholase reactions such as those reported here are rare.[6]

The VO(psal)(L) species are inert to oxygen in solution. This is somewhat surprising since electrochemically the diol ligand in **3** is more easily oxidizable than that in **2**. It is believed that the hydrogen atom of the coordinated HL^- ligand plays a crucial role in the initial binding of the oxygen molecule. Oxygen binding via hydrogen bridges has been documented among metalloenzymes.[26] The propensity of the coordinated HL^- hydrogen to form a strong hydrogen bond was cogently revealed in the structures of the VO(xsal)(HL) species (Figure 4). The intimate mechanism of the subsequent events in the oxidation process, eq 1, is unclear at present.

Concluding Remarks

The main findings of the present work will now be recapitulated. Esters of the type VO(xsal)(HL), **2**, incorporating the rarely observed chelation of monoionized aromatic 1,2-diols have been isolated and characterized along with the diionized diol esters VO(psal)(L), **3**. The coligand influences the protic and electronic nature of the diol fragment, which is bonded as a catechol in **2** and as a catechol−semiquinone hybrid in **3**.

The type **2** species with chiral amino acid residues occur exclusively in the endo form, which is selectively stabilized by the folded structure of the salicylaldimine coligand. The phenolic OH group in **2** is strongly hydrogen bonded to a carboxylic oxygen atom of a neighboring molecule, thus forming a chain in the lattice.

The type **2** species are electrochemically more difficult to reduce ($V^V \rightarrow V^{IV}$) as well as to oxidize (catecholate → semiquinonate) than the type **3** species. Yet only **2** is oxidized spontaneously and quantitatively by O_2 in solution furnishing the corresponding quinone, Lq, and $V_2O_3(xsal)_2$, which is reconverted to **2** upon addition of H_2L. These reactions provide a method for catalytic oxidation (catecholase reaction) of H_2L to Lq. It is proposed that the O_2 molecule is

(25) (a) *Bioinorganic Chemistry of Copper*; Karlin, K. D., Tyeklar, Z., Eds.; Chapman and Hall: New York, 1993. (b) Solomon, E. I.; Baldwin, M. J.; Lowery, M. D. *Chem. Rev.* **1992**, *92*, 521. (c) Kitajima, N.; More-Oka, Y. *Chem. Rev.* **1994**, *94*, 734.

(26) (a) Perutz, M. F.; Fermi, G.; Luisi, B.; Shaanan, B.; Liddington, R. C. *Acc. Chem. Res.* **1987**, *20*, 309. (b) Shaanan, B. *J. Mol. Biol.* **1983**, *171*, 31. (c) Stenkamp, R. E. *Chem. Rev.* **1994**, *94*, 715.

initially attached to **2** via hydrogen bonding with the coordinated HL^- ligand. Further work is in progress.

Experimental Section

Materials. $V^{IV}O(xsal)(H_2O)$,[17] $VO^V(xsal)(OMe)(HOMe)$,[18] $VO(acac)_2$,[19] and tetraethylammonium perchlorate (TEAP)[27] were prepared by reported methods. 2-Picolylamine, salicylaldehyde, and catechols were obtained from Fluka and Aldrich. All other chemicals and solvents were of analytical grade and were used as received.

Physical Measurements. UV−vis spectral measurements were carried out with a Shimadzu UVPC 1601 spectrometer fitted with thermostated cell compartments. IR spectra were measured with a Nicolet Magna IR750 Series II spectrometer. Proton NMR and ^{51}V NMR spectra were respectively recorded on a Bruker FT 300 MHz spectrometer and a Varian spectrometer at 78.8 MHz ($VOCl_3$ external reference). The atom numbering scheme used for ^1H NMR is the same as that used in crystallography. Spin−spin structures are abbreviated as follows: s, singlet; d, doublet; t, triplet; m, multiplet; br, broad. Cyclic voltammetry was performed (scan rate, 50 mVs^{-1}) in MeCN solution (0.1 M TEAP) under nitrogen atmosphere on a PAR 370-4 electrochemical system,[28] using a platinum working electrode with reference to a saturated calomel electrode (SCE). A Perkin-Elmer 2400 elemental analyzer was used for microanalysis (C, H, N).

Preparation of Esters. The VO(xsal)(HL) and VO(psal)(L) esters were prepared by general methods starting from $VO(xsal)(H_2O)$/VO(xsal)(OMe)(HOMe) and $VO(acac)_2$, respectively. Details are given below for representative cases.

VO(vsal)(HL^2), 2f. To a stirred methanolic solution (10 mL) of $VO(vsal)(H_2O)$ (0.20 g, 0.66 mmol) was added a slight excess of H_2L^2 (0.219 g, 0.99 mmol). The deep blue solution thus obtained was kept undisturbed at room temperature to evaporate slowly under nitrogen atmosphere. After 12 h a dark crystalline solid was obtained, which was washed with hexane (to remove excess H_2L^2) and then with a minimum volume of cold methanol. It was finally dried over fused $CaCl_2$ in vacuo. Yield: 0.240 g (72%). Anal. Calcd for $C_{26}H_{34}NO_6V$: C, 61.53; H, 6.75; N, 2.76. Found: C, 61.57; H, 6.68; N, 2.72. UV−vis (λ_{max}, nm (ϵ, M^{-1} cm^{-1}) Me_2CO solution): 647 (3650); 376 (1430). IR (KBr, cm^1): $\nu_{(V=O)}$ 996, $\nu_{(CH=N)}$ 1644; $\nu_{(OH)}$ 2580. ^1H NMR (δ (*J*, Hz) $(CD_3)_2CO$): 4.23 (H(2), br); 8.91 (H(3), s); 7.71 (H(5), d, 7.6); 7.01 (H(6), t, 6.7); 7.59 (H(7), t, 7.4); 6.83 (H(8), d, 8.4); 6.97 (H(11), s); 6.62 (H(13), s); 2.79 (H(16), br); 1.11 (C(16)Me_2, d, 6.7); 1.19 (C(19)Me_3, s); 1.51 (C(23)Me_3, s); 10.03 (OH, br).

VO(asal)(HL^2), 2e. Here VO(asal)(OMe)(HOMe) was used as the starting material in place of $VO(asal)(H_2O)$ and the reaction medium was acetonitrile instead of methanol. The rest of the procedure remains the same as above. Yield: 82%. Anal. Calcd for $C_{24}H_{30}NO_6V$: C, 60.12; H, 6.31; N, 2.92. Found: C, 60.23; H, 6.39; N, 3.10. UV−vis (λ_{max}, nm (ϵ, M^{-1} cm^{-1}) Me_2CO solution): 641 (3380); 373 (1290). IR (KBr, cm^{-1}): $\nu_{(V=O)}$ 991; $\nu_{(CH=N)}$ 1619; $\nu_{(OH)}$ 2475. ^1H NMR (δ (*J*, Hz) $(CD_3)_2CO$): 4.69 (H(2), br); 8.96 (H(3), s); 7.68 (H(5), d, 7.4); 7.01 (H(6), t, 7.6); 7.58 (H(7), t, 7.2); 6.85 (H(8), d, 8.2); 6.98 (H(11), s); 6.67 (H(13), s); 1.79 (C(2)Me, br); 1.21 (C(17)Me_3, s); 1.51 (C(21)Me_3, s); 10.15 (OH, br).

VO(gsal)(HL^2), 2d. The method is the same as for **2f**. Yield: 76%. Anal. Calcd for $C_{23}H_{28}NO_6V$: C, 59.36; H, 6.06; N, 3.01. Found: C, 59.48; H, 5.97; N, 3.09. UV−vis (λ_{max}, nm (ϵ, M^{-1} cm^{-1}) Me_2CO solution): 638 (3530); 371 (1370). IR (KBr, cm^{-1}): $\nu_{(V=O)}$ 993; $\nu_{(CH=N)}$ 1630; $\nu_{(OH)}$ 2533. ^1H NMR (δ (*J*, Hz) $(CD_3)_2CO$): 4.70 (H(2A), br); 5.22 (H(2B), br); 8.97(H(3), s); 7.72 (H(5), d, 7.8); 7.02 (H(6), t, 7.4); 7.62 (H(7), t, 7.8); 6.87 (H(8), d, 8.4); 7.01 (H(11), s); 6.74 (H(13), s); 1.24 (C(16)Me_3, s); 1.53 (C(20)-Me_3, s); 10.28 (OH, br).

VO(vsal)(HL^1), 2c. The procedure is similar to that for **2d** but the initial washing of the product was done with water (to remove excess H_2L^1) and then with a minimum volume of cold methanol. Yield: 75%. Anal. Calcd For $C_{18}H_{18}NO_6V$: C, 54.69; H, 4.59; N, 3.54. Found: C, 54.78; H, 4.41; N, 3.67. UV−vis (λ_{max}, nm, Me_2-CO solution): 602; 378. IR (KBr, cm^{-1}): $\nu_{(V=O)}$ 997; $\nu_{(CH=N)}$ 1612; $\nu_{(OH)}$ 2533. ^1H NMR (δ (*J*, Hz) $(CD_3)_2SO$): 4.23 (H(2), br); 8.94 (H(3), s); 7.69 (H(5), d, 7.3); 6.96 (H(6), t, 6.0); 7.51 (H(7), t, 8.3); 6.79 (H(8), d, 8.4); 6.58 (H(11), H(12), m); 6.70 (H(13), H(14), m); 3.14 (H(16), m); 1.13 (C(16)Me(17), d, 6.6); 1.02 (C(16)Me-(18), d, 6.7).

VO(asal)(HL^1), 2b. The procedure is the same as for **2c**. Yield: 80%. Anal. Calcd for $C_{16}H_{14}NO_6V$: C, 52.33; H, 3.84; N, 3.81. Found: C, 52.47; H, 3.95; N, 3.91. UV−vis (λ_{max}, nm, Me_2 CO solution): 591; 373. IR (KBr, cm^{-1}): $\nu_{(V=O)}$ 998; $\nu_{(CH=N)}$ 1619; $\nu_{(OH)}$ 2535. ^1H NMR (δ (*J*, Hz) $(CD_3)_2SO$): 4.70 (H(2), br); 9.02 (H(3), s); 7.70 (H(5), d, 6.8); 6.99 (H(6), t, 6.0); 7.57 (H(7), t, 8.3); 6.83 (H(8), d, 8.2); 6.59 (H(11), H(12), m); 6.71 (H(13), H(14), m); 1.68 (C(2)Me, d, 5.3).

VO(gsal)(HL^1), 2a. The procedure is the same as for **2c**. Yield: 92%. Anal. Calcd for $C_{15}H_{12}NO_6V$: C, 51.01; H, 3.42; N, 3.97. Found: C, 50.87; H, 3.36; N, 3.82. UV−vis (λ_{max}, nm, Me_2CO solution): 578; 376. IR (KBr, cm^{-1}): $\nu_{(V=O)}$ 992; $\nu_{(CH=N)}$ 1627; $\nu_{(OH)}$ 2492. ^1H NMR (δ (*J*, Hz) $(CD_3)_2SO$): 4.71 (H(2A), d, 18.9); 5.16 (H(2B), d, 15.9); 8.98 (H(3), s); 7.33 (H(5), d, 6.0); 7.02 (H(6), t, 6.0); 7.61 (H(7), t, 6.6); 6.91 (H(8), d, 7.8); 6.67 (H(11), H(12), m); 6.78 (H(13), H(14), m).

VO(psal)(L^1), 3a. To an oxygen-saturated methanolic solution (20 mL) of $VO(acac)_2$ (0.10 g, 0.38 mmol) and Hpsal (0.08 g, 0.38 mmol) was added H_2L^1 (0.084 g, 0.38 mmol). The violet solution was stirred for 2 h and then kept undisturbed to evaporate at room temperature in air. The dark violet crystalline product that deposited within 1 day was filtered off, washed with cold methanol, and dried over fused $CaCl_2$ in vacuo. Yield: 0.128 g (88%) Anal. Calcd for $C_{19}H_{15}N_2O_4V$: C, 59.08; H, 3.91; N, 7.25. Found: C, 59.17; H, 3.95; N, 7.32. UV−vis (λ_{max}, nm (ϵ, M^{-1} cm^{-1}) Me_2CO solution): 850 (4620); 525 (3600); 375 (2950). IR (KBr, cm^{-1}): $\nu_{(V=O)}$ 950; $\nu_{(CH=N)}$1622. ^1H NMR (δ (*J*, Hz) $CDCl_3$): 8.46 (H(1), d, 5.1); 7.54 (H(2), H(4), H(9), H(11), m); 7.91 (H(3), t, 6.6); 5.59 (H(6A), d, 19.2); 5.44 (H(6B), d, 18.9); 8.54 (H(7), s); 6.83 (H(10), t, 7.2); 7.06 (H(12), d, 8.7); 6.72 (H(15), H(18), m); 6.30 (H(16), H(17), m).

VO(psal)(L^2)·H_2O. 3b. The procedure is the same as for **3a**. Yield: 89%. Anal. Calcd for $C_{27}H_{33}N_2O_5V$: C, 62.79; H, 6.44; N, 5.42. Found: C, 62.86; H, 6.47; N, 5.51. UV−vis (λ_{max}, nm (ϵ, M^{-1} cm^{-1}) Me_2CO solution): 855 (4760); 550 (5150); 375 (2900). IR (KBr, cm^{-1}): $\nu_{(V=O)}$ 960; $\nu_{(CH=N)}$ 1625. ^1H NMR (δ (*J*, Hz) $CDCl_3$): 8.46 (H(l), H(7), br); 7.44(H(2), H(4), H(11), m); 7.88 (H(3), t, 7.5); 5.59 (H(6A), d, 18.0); 5.38 (H(6B), d, 18.0); 7.34 (H(9), d, 6.0); 6.75 (H(10), t, 7.5); 7.04 (H(12), d, 9.0); 6.23 (H15), H(17), br); 1.52 (C(24)Me_3, br), 1.20 (C(20)Me_3, br).

Reaction of VO(vsal)(HL^2) with Oxygen: Isolation of Products. A solution of **2f** (0.10 g, 0.2 mmol) in O_2-saturated acetone solution (50 mL) was taken in a two-necked flask fitted with a balloon filled with O_2 and stirred for 10 h. At the end of the reaction (reaction solution yellowish brown) H_2L^2 (0.044 g, 0.2 mmol) was

(27) Sawyer, D. T.; Roberts, J. L., Jr. *Experimental Electrochemistry for Chemists*; Wiley: New York, 1974; p 212.
(28) Lahiri, G. K.; Bhattacharya, S.; Ghosh, B. K.; Chakravorty, A. *Inorg. Chem.* **1987**, *26*, 4324.

added and the original deep blue color was reestablished. This solution was again bleached with O_2 as above and two more instalments (each 0.044 g) of H_2L^2 were added repeating the events. The solvent was then removed and the solid thus obtained was dried in a vacuum over fused $CaCl_2$. The dry mass was extracted with petroleum ether (60−80 °C) leaving pure $V_2O_3(vsal)_2$ as the residue. Removal of solvent from the filtrate afforded the quinone, Lq^2. The observed yields of Lq^2 and $V_2O_3(vsal)_2$ are 0.169 and 0.056 g, respectively. Theoretical yields for complete conversion are 0.174 and 0.058 g, respectively. The complex $V_2O_3(vsal)_2$ has been characterized. Anal. Calcd for $C_{24}H_{26}N_2O_9V_2$: C, 48.99; H, 4.45; N, 4.76. Found: C, 49,03; H, 4.52; N, 4.71. IR (KBr, cm^{-1}): $\nu_{(V=O)}$ 992; $\nu_{(CH=N)}$ 1686. ^1H NMR (δ (*J*, Hz) $CDCl_3$): 4.02 (H(2A), br); 4.25 (H(2B), br); 8.44 (H(3), s); 7.68 (H(5), d, 6.0); 7.11 (H(6), t, 7.5); 7.64 (H(7), t, 9.0); 7.09 (H(8), d, 9.0); 2.32, 2.54 (H(10), m); 0.97, 1.04 ($C(10)Me_2$, d, 6.0). The quinone, Lq^2, was characterized by ^1H NMR.

Synthesis of VO(vsal)(HL^2) from $V_2O_3(vsal)_2$. To a stirred acetone solution (30 mL) of $V_2O_3(vsal)_2$ (0.10 g, 0.17 mmol) was added H_2L^2 (0.076 g, 0.34 mmol) under N_2 atmosphere. After 0.5 h the reaction mixture was concentrated to 10 mL and then kept at 4 °C. The precipitate thus obtained was filtered off and washed with hexane and dried in vacuo affording 0.079 g (92%) of VO(vsal)(HL^2).

Rate Measurements. The initial O_2 concentration in O_2-saturated acetone determined by using an oxygen-sensitive electrode was found to be 0.90×10^{-3} M. The concentration of the complex was varied in the range $(1-4) \times 10^{-5}$ M. The spectrum of a solution of VO(vsal)(HL^2) in O_2-saturated acetone (295 K) was followed spectrophotometrically (quartz cell path length, 1 cm) by measuring the absorbance (A_t) at 647 nm as a function of time, *t*. The absorbance A_α at the end of 24 h of reaction was also measured. The values of k_{obs} were obtained from the slope of the linear plot of $-\ln(A_\alpha - A_t)$ versus *t*. At substrate concentrations of 3.90×10^{-5}, 2.95×10^{-5}, and 1.65×10^{-5} M the k_{obs} values were 5.64×10^{-4}, 5.70×10^{-4}, and 5.58×10^{-4} s^{-1} (average 5.64×10^{-4} s^{-1}), respectively.

X-ray Structure Determination. Crystals of VO(gsal)(HL^1), VO(vsal)(HL^2), and VO(psal)(L^2)·H_2O were grown by slow evaporation of their solutions in methanol. Cell parameters were determined by the least-squares fit of 30 machine-centered reflections ($14 \le 2\theta \le 28°$). Data were collected by the ω-scan technique in the 2θ range 3−50° for all three complexes on a Siemens R3m/V four-circle diffractometer with graphite-monochromated Mo Kα (λ = 0.71073 Å) radiation at 293 K. Two check reflections after each 198 reflections showed no significant intensity reduction for any of the crystals. Data were corrected for Lorentz−polarization effects and empirical absorption correction was performed on each set of data on the basis of azimuthal scans[29] of six reflections.

Table 5. Crystallographic Data for VO(gsal)(HL^1), **2a**, VO(vsal)(HL^2), **2f**, and VO(psal)(L^2)·H_2O, **3b**

	2a	**2f**	**3b**
chemical formula	$C_{15}H_{12}NO_6V$	$C_{26}H_{34}NO_6V$	$C_{27}H_{33}N_2O_5V$
fw	353.20	507.48	516.49
space group	$P2_1/n$ (no. 14)	$R3$ (no.146)[a]	$P2_1/n$ (no. 14)
a, Å	10.436(4)	23.754(5)	9.382(7)
b, Å	9.757(2)	23.754(5)	11.617(5)
c, Å	14.410(5)	12.836(3)	23.979(11)
β, deg	101.70(3)		97.31(5)
V, Å^3	1436.8(8)	6272(2)	2592(2)
Z	4	9	4
T, °C	20	20	20
λ, Å	0.71073	0.71073	0.71073
ρ_{calcd}, mg m^{-3}	1.633	1.209	1.323
μ(Mo Kα), cm^{-1}	7.22	3.92	4.22
$R1$,[b] w$R2$[c] [$I > 2\sigma(I)$]	0.0577, 0.1447	0.0515, 0.1344	0.0589, 0.1402
goodness of fit on F^2	1.081	1.089	1.079

[a] Hexagonal axes. [b] $R1 = \sum|F_o| - |F_c|/\sum|F_o|$. [c] $wR2 = [\sum w(F_o^2 - F_c^2)^2/\sum w(F_o^2)^2]^{1/2}$.

All calculations of data reduction, structure solution, and refinement were done with the programs of SHELXTL, Version 5.03.[30] The three structures were solved by direct methods and were refined by full-matrix least-squares on F^2. All non-hydrogen atoms were refined anisotropically. The number of hydrogen atoms located directly in difference Fourier maps for compounds VO(gsal)(HL^1) and VO(vsal)(HL^2) was 8 and 23, respectively. The remaining hydrogen atoms were included in calculated positions. Significant crystal data are listed in Table 5.

Acknowledgment. We thank the Department of Science and Technology and Council of Scientific and Industrial Research, New Delhi, for financial support. Thanks are due to Drs. S. P. Rath and K. K. Rajak for performing certain preliminary experiments.

Supporting Information Available: For VO(gsal)(HL^1), VO(vsal)(HL^2) and VO(psal)(L^2)·H_2O crystallographic data, atomic coordinates and equivalent isotopic coefficients, complete bond distances and angles, anisotropic thermal parameters, hydrogen atom positional parameters. The crystallographic files, in CIF format are available free of charge via the Internet at http://www.pubs.acs.org.

IC020259D

(29) North, A. C. T.; Phillips, D. C.; Mathews, F. S. *Acta Crystallogr., Sect. A* **1968**, *24*, 351.
(30) Sheldrick, G. M. *SHELXTL*, Version 5.03; Siemens Analytical Instruments, Inc: Madison, WI, 1994.